Effects of Transpiration and Changing Diameter on Heat and Mass Transfer to Spheres

P. L. T. BRIAN and H. B. HALES

Massachusetts Institute of Technology, Cambridge, Massachusetts

Mass transfer to spheres suspended in an agitated liquid has been studied both experimentally and theoretically. Finite-difference solutions are obtained for mass transfer from a sphere to a fluid flowing past it in steady viscous flow. The effects of a transpiration velocity at the surface of the sphere and of a continuously changing sphere diameter are included. A normalized presentation of these effects is quite insensitive to the bulk flow Peclet number. When these theoretical corrections for transpiring and shrinking spheres are applied to the mass transfer data for ice spheres that are melting in an agitated brine bath, the corrected mass transfer coefficients are brought into agreement with a generalized correlation published elsewhere. This agreement suggests that the theoretical results apply, with reasonable accuracy, to a shrinking and transpiring sphere that is suspended in a turbulent liquid.

Rates of mass and heat transport to small particles suspended in agitated liquids are important in many chemical processes that involve dissolution, crystallization, and heterogeneous chemical reaction. The transport process often proceeds with a continuously changing particle size and is therefore transient in nature. Furthermore, there is often a finite radial fluid velocity at the particle surface, and this transpiration velocity can affect the transport process. In much of the literature the effects of transpiration and of a changing particle size have been assumed to have a negligible influence upon the transport rate to suspended particles. This assumption is probably acceptable in many situations, but in others it may not have been valid.

The purpose of this work is to present a theoretical analysis of these effects. The equation of continuity for mass or heat diffusion is solved numerically for a sphere in a steady unidirectional viscous fluid flow. Solutions are obtained which include the effects of transpiration at the particle surface and a continuously changing particle radius. Generalized graphs of these results are then compared with experimental results for transport to particles freely suspended in a turbulent liquid.

THEORY

The theoretical analysis to be presented involves a numerical solution of the partial differential equation describing the transport of mass from a sphere:

$$\frac{\partial c}{\partial t} + v_r \frac{\partial c}{\partial r} + \frac{v_\theta}{r}\frac{\partial c}{\partial \theta} = D\left[\frac{1}{r^2}\frac{\partial}{\partial r}\left(r^2\frac{\partial c}{\partial r}\right) + \frac{1}{r^2 \sin\theta}\frac{\partial}{\partial \theta}\left(\sin\theta\frac{\partial c}{\partial \theta}\right)\right] \quad (1)$$

Heat transfer nomenclature is equally valid, but the discussion will be presented in terms of mass transfer nomenclature. To describe the transport with unidirectional flow past a sphere, Equation (1) is employed with the following boundary conditions:

$$\left.\begin{aligned} &c = c_b \text{ as } r \to \infty \\ &c = c_s \text{ at } r = R \end{aligned}\right\} (c_b, c_s = \text{constants})$$
$$\frac{\partial c}{\partial \theta} = 0 \text{ at } \theta = 0 \text{ and } \theta = \pi \quad (2)$$

Equation (1) assumes that the concentration field is axisymmetric, the fluid is incompressible, the diffusivity is constant throughout the region of interest, and, in the case of heat transfer, that viscous energy dissipation is negligible.

The model further assumes the velocity profile existing around the sphere to be that which occurs with steady Stokes flow past a sphere of constant radius, thus

$$\frac{v_r}{v_b} = -\left(1 - \frac{3}{2}\frac{R}{r} + \frac{1}{2}\frac{R^3}{r^3}\right)\cos\theta + \frac{(v_r)_s}{v_b}\frac{R^2}{r^2}$$
$$\frac{v_\theta}{v_b} = \left(1 - \frac{3}{4}\frac{R}{r} - \frac{1}{4}\frac{R^3}{r^3}\right)\sin\theta \quad (3)$$

The last term in the first of these equations accounts for the effect of a transpiration velocity at the particle surface (*10*). For the case of a sphere of changing radius, this velocity profile corresponds to the steady state profile at the instantaneous sphere radius, and thus it neglects transient effects in momentum transfer. This should be valid if the momentum diffusivity is much greater than the diffusivity for the transport process under consideration, that is, for a large Schmidt or Prandtl number.

Equation (1) is not in a convenient form for numerical solution because the region of interest extends to infinity, and hence new variables are defined as

$$X \equiv \frac{c - c_b}{c_s - c_b}; \quad T \equiv \frac{Dt}{R_i^2}; \quad A \equiv \frac{R}{r} \quad (4)$$

Both X, the dimensionless concentration, and A, the dimensionless inverse radial distance, vary between zero and unity. With these new variables and the velocities of Equation (3), Equation (1) becomes

$$\left(\frac{R}{R_i}\right)^2 \frac{\partial X}{\partial T} = \left[-\frac{N_{Pe}}{2}\left(A^2 - \frac{3}{2}A^3 + \frac{1}{2}A^5\right)\cos\theta + \frac{N_{PeT}}{2}A^4 - \frac{N_{PeR}}{2}A\right]\frac{\partial X}{\partial A} + \left[-\frac{N_{Pe}}{2}\left(A - \frac{3}{4}A^2 - \frac{1}{4}A^4\right)\sin\theta\right.$$

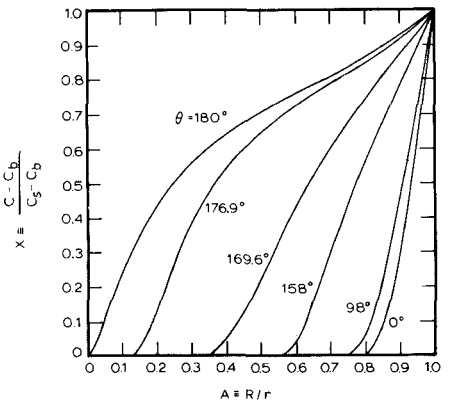

Fig. 1. Concentration profile around sphere, steady viscous flow, $N_{Pe} = 1{,}000$.

$$+ A^2 \cot\theta \Big] \frac{\partial X}{\partial \theta} + A^4 \frac{\partial^2 X}{\partial A^2} + A^2 \frac{\partial^2 X}{\partial \theta^2} \quad (5)$$

N_{Pe} is the bulk flow Peclet number, $2Rv_b/D$, based on the bulk flow velocity, v_b; N_{PeT} is the transpiring Peclet number $2R(v_r)_s/D$, based on the transpiration velocity $(v_r)_s$; and N_{PeR} is the radial Peclet number, $(2R/D)(dR/dt)$, based upon the time rate of change of the particle radius. The transpiration velocity, $(v_r)_s$, is defined as the radial velocity at the particle surface, relative to a fixed point such as the center of the sphere. Hence, for crystallization and dissolution processes a nonzero transpiring Peclet number results only when a density difference exists between the solid and liquid phases.

With the change of coordinates, the boundary conditions of Equation (2) become

$$X = 0 \text{ at } A = 0$$
$$X = 1 \text{ at } A = 1 \quad (6)$$
$$\frac{\partial X}{\partial \theta} = 0 \text{ at } \theta = 0 \text{ and } \theta = \pi$$

The local mass transfer coefficient, k_L, is defined by

$$k_L(c_s - c_b) = -D \left.\frac{\partial c}{\partial r}\right|_{r=R} \quad (7)$$

and the local mass transfer Nusselt number at any point on the surface is given by

$$(N_{Nu})_L = 2 \left.\frac{\partial X}{\partial A}\right|_{A=1} \quad (8)$$

The solution of these equations by finite-difference methods proved to be difficult, and stable numerical solutions were obtained only after an additional transformation of variables. This transformation employed, as an independent variable, a function of A and θ which had been developed as an approximation to the steady state concentration profile $X(A, \theta)$. This appears to be a powerful technique which may have general applicability. The finite-difference method was a modification of the method suggested by Brian (5). The details of the transformation and the numerical method are given elsewhere (*10*). The convergence of the finite-difference method was tested by decreasing the increments in the distance net and, for transient solutions, in the time step. These convergence tests indicated that the results are convergent to within 1% in Figure 2 and to within 3 to 4% in Figures 3 through 6. The details are given in reference *10*.

Steady Transport in Stokes Flow

Perhaps the simplest solution to Equation (5) results when both the transpiring and the radial Peclet numbers are zero. Such a solution not only provides a basis of comparison for the solutions obtained with transpiration and changing particle radius, but it also provides an exact representation of transport from spheres in steady flow at Reynolds numbers less than unity. Steady state concentration profiles obtained by the numerical solution at a flow Peclet number equal to 1,000 are shown in Figure 1. It can be seen that a maximum transport rate occurs at the stagnation point, $\theta = 0$, but the rate decreases only slightly over the entire front half of the sphere. However, toward the back of the sphere, the transport rate falls off substantially. The solution for steady state diffusion from a sphere into an infinite stagnant medium corresponds to $N_{Pe} = 0$, and the concentration profile in this case is simply $X = A$ at all values of θ. It can be seen in Figure 1 that with $N_{Pe} = 1{,}000$ the profile at $\theta = 180°$ has a slope at $A = 1$ which is less than unity, and thus the transport coefficient at the back of the sphere is less than that for a stagnant medium ($N_{Nu}^* = 2$). In this region the convective velocities actually increase the boundary layer thickness.

Similar concentration profiles were found for other Peclet numbers. At low flow Peclet numbers, the concentration profile approaches $X = A$, but as flow is increased, the curves describing the solution at various angles around the sphere become more and more widely separated. Transport rates at the front of the sphere are increased, while those at the back are decreased regardless of the magnitude of the convective velocity. The resulting area-averaged Nusselt numbers, N_{Nu}^*, are shown in Table 1 and Figure 2. The solid curve in Figure 2, which describes the numerical solution, can be represented within 5% by the simple empirical expression:

$$[(N_{Nu}^*)^2 - 4]^{1/2} = 1.1\, N_{Pe}^{1/3} \quad (9)$$

Figure 2 also shows the viscous flow transport results of other investigators. At low values of the flow Peclet number, the work of Acrovis and Taylor (*1*) is representative of the work done by several others (*3, 4, 8, 9, 11*).

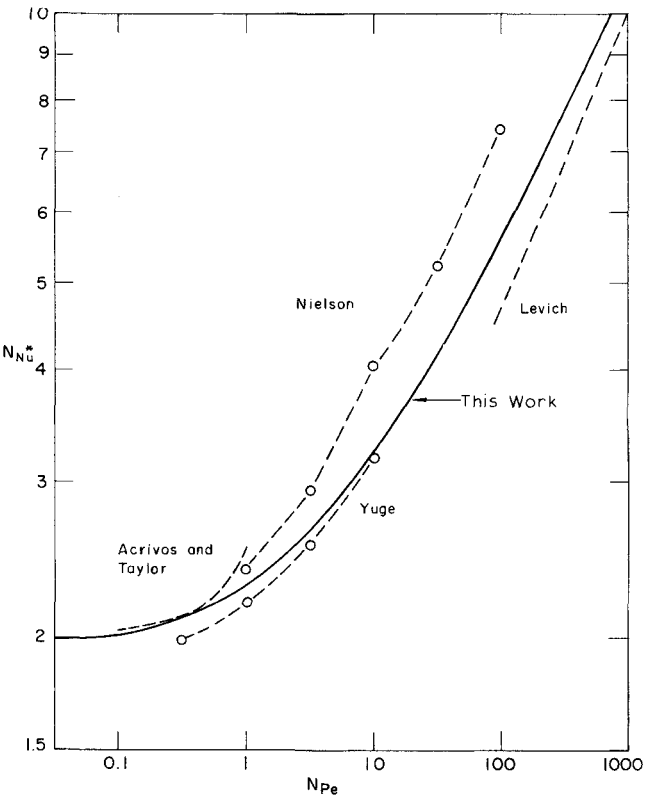

Fig. 2. Steady state transport around a sphere, viscous flow, $N_{PeR} = N_{PeT} = 0$.

TABLE 1. STEADY TRANSPORT TO A SPHERE IN STOKES FLOW, $N_{PeT} = N_{PeR} = 0$

N_{Pe}	N^*_{Nu}
0.03	2.01
0.1	2.02
0.3	2.12
1	2.30
3	2.62
10	3.25
30	4.12
100	5.62
300	7.65
1,000	11.01
10,000	22.87

Each study used a perturbation technique valid for $N_{Pe} \to 0$, and the results take the form of a power series in N_{Pe}, such as

$$N_{Nu}^* = 2 + \frac{1}{2} N_{Pe} + \ldots \qquad (10)$$

differing slightly in succeeding terms. For increased values of N_{Pe} Friedlander (*8*) used the von Karman integral technique to obtain $N_{Nu}^* = 0.89\ N_{Pe}^{1/3}$. Similar results are given by Bowman, et al. (*2*). Levich's solution (*12*), used by Friedlander (*9*), involves the analytic solution of the partial differential equation with a simplified velocity profile and is probably more accurate. This solution, $N_{Nu}^* = 0.997\ N_{Pe}^{1/3}$, appears in Figure 2. These solutions, however, assume no angular diffusion.

Friedlander's solution based on the von Karman integral is also valid in the intermediate-Peclet range, but perhaps a more accurate solution in this area results from the work of Yuge (*15*). Yuge assumed X to be a power series in θ, with each coefficient an arbitrary function of $1/A$. He then numerically solved the first three resulting ordinary differential equations for these coefficients.

Each of these solutions involves simplifying assumptions, either in the partial differential equation, the velocity profile, or the solution itself. The transport coefficients derived by a finite-difference solution of Equation (5), however, can be obtained without this type of simplification. Neilson (*14*) used a relaxation technique to solve the equation of continuity, but he gives no details of his numerical scheme nor its behavior. Convergence tests (*10*) indicate that the present finite-difference results are convergent to within 1%, thus they are presumed to be more accurate than the other results shown in Figure 2.

Transport from a Transpiring Sphere

Consider first the case of a sphere of constant radius in an infinite stagnant medium, but with a steady transpiration flow through the surface of the sphere. In this case, N_{Pe} and N_{PeR} are both zero, and Equation (5) can be solved analytically (*10*) to give

$$N_{Nu} = \frac{N_{PeT}}{\exp\,(N_{PeT}/2) - 1} \qquad (11)$$

or

$$\frac{N_{Nu}}{N_{Nu}^*} = \frac{N_{PeT}/N_{Nu}^*}{\exp(N_{PeT}/N_{Nu}^*) - 1} \qquad (12)$$

where N_{Nu}^* is the Nusselt number which would result without transpiration. The form of Equation (12) for a sphere is identical to the result obtained by Mickley et al. (*13*) for a film theory model of a transpiring boundary layer on a flat plate. It is important to note that, in this work, the mass transfer coefficient is defined by Equation (7), and represents diffusive transport only. With transpiration present, the convective flux must be added to the diffusive flux so that the total flux can be obtained.

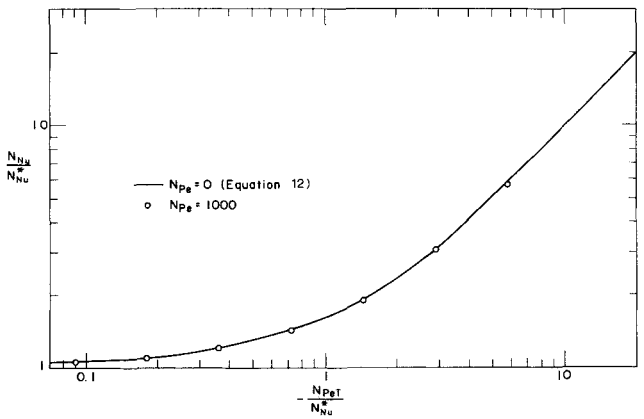

Fig. 3. Transport from a transpiring sphere (flow into spherical surface).

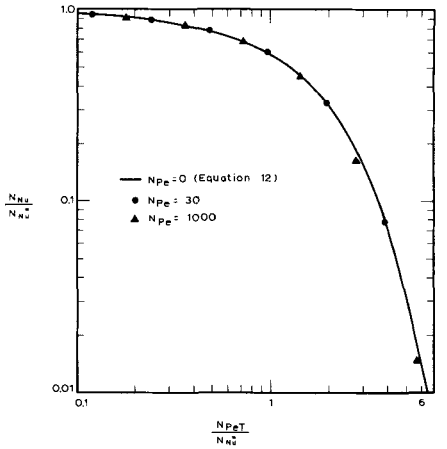

Fig. 4. Transport from a transpiring sphere (flow from spherical surface).

Equation (12) is plotted in Figures 3 and 4 for inward and outward transpiration respectively (solid curves). Transpiration flow inward results in a thinning of the concentration boundary layer and yields an increased mass transfer coefficient. The opposite is true for an outward transpiration flow.

For the case of a sphere of constant radius immersed in a steady viscous flow and with transpiration through its surface, N_{PeR} is zero, but N_{Pe} and N_{PeT} are nonzero. For this case, finite-difference solutions to Equation (5) were obtained for bulk flow Peclet numbers of 30 and 1,000. These results are plotted in Figures 3 and 4 and are seen to lie very close to the curves representing Equation (12). Normalizing the variables, as in Figures 3 and 4 and Equation (12), evidently gives results essentially independent of the value of the bulk flow Peclet number. The normalizing variable N_{Nu}^* is the Nusselt number in the absence of transpiration but at the same bulk flow Peclet number. When $N_{Pe} = 0$, N_{Nu}^* is equal to 2.

Transport from a Sphere of Changing Diameter

First consider the case in which the bulk flow and transpiring Peclet numbers are both zero. An analytical solution can be obtained for the case of a growing sphere, which corresponds to positive values of N_{PeR}. Such a solution was first obtained by Frank (*7*); it can also be obtained from Equation (5) by assuming that N_{PeR} does not change with time and seeking a time-independent solution. The result is

$$N_{Nu} = \frac{2}{1 - (1/2)\sqrt{\pi N_{PeR}}\ \exp(N_{PeR}/4)\ \operatorname{erfc}(\sqrt{N_{PeR}}/2)} \qquad (13)$$

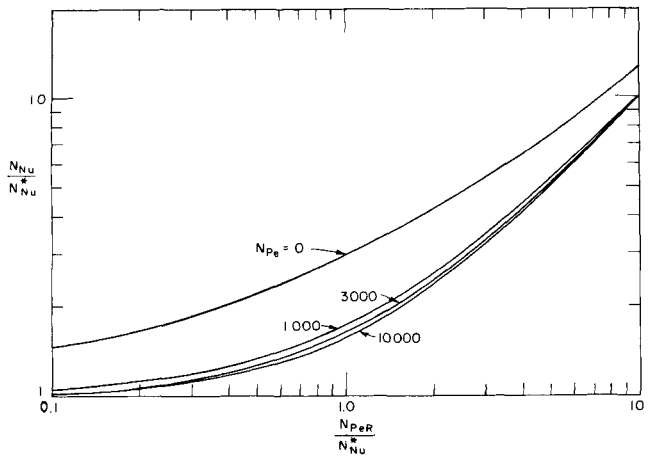

Fig. 5. Transport from a growing sphere.

Equation (13) is plotted as the uppermost curve in Figure 5 in normalized coordinates analogous to those employed in Figures 3 and 4. The normalizing parameter is N_{Nu}^*, which is the Nusselt number for a sphere of constant diameter at the same bulk flow Peclet number.

Figure 5 shows that the transport coefficient to a growing sphere in a stagnant medium ($N_{Pe} = 0$) at large values of N_{PeR}/N_{Nu}^* is greater than for a sphere of constant diameter. This group may be thought of as the diffusion time-constant for the boundary layer divided by the time required for the sphere radius to grow equal to the amount of the boundary layer thickness. When this ratio is large, the concentration profile is quite steep as it cannot spread out fast enough by diffusion to keep ahead of the growing sphere radius.

The analogous solution describing transport to a melting, or dissolving, sphere has not been obtained analytically, and analytical solutions have not been published for transport from either a growing or a shrinking sphere with a transverse flow past the particle. The solution given by Equation (13) is unique because the resulting Nusselt number is independent of time. In general, the transient nature of the transport process for a growing or shrinking sphere results in a time-dependent Nusselt number and a time-dependent radial Peclet number. But while N_{Nu} and N_{PeR} generally vary with time, stoichiometric relationships often require that their ratio remain constant. Before proceeding with numerical solutions for shrinking and growing spheres in a steady viscous bulk flow, these stoichiometric relationships will first be explored.

For dissolution and crystallization processes which are controlled by the rate of heat or mass transfer, the Nusselt number and the radial Peclet number can be related to each other by the mass or energy balance. For example, in dissolving a solid sphere in a liquid, or in crystallizing a solute species from a liquid solution, a mass balance yields

$$-\rho_s \frac{dR}{dt} = k\,(c_s - c_b) - \frac{\rho_s}{\rho_L} c_s \frac{dR}{dt} \tag{14}$$

and the radial Peclet number is thus related to the mass transfer Nusselt number through the following:

$$N_{Nu} = \alpha\ N_{PeR} \tag{15}$$

where

$$\alpha = \frac{\rho_s - c_s\rho_s/\rho_L}{c_b - c_s} \tag{16}$$

Similarly, for the freezing or melting of an isothermal solid sphere, the first law of thermodynamics relates the heat transfer Nusselt number to the radial Peclet number by Equation (15) with

$$\alpha = \frac{\lambda\rho_s}{C_p\rho_L(T_s - T_b)} \tag{17}$$

These equations do not apply to the case in which the local transport coefficient varies with position around the sphere so that transport-limited dissolution or crystallization changes the particle to a nonspherical shape. Rather, these equations assume that the particle remains spherical, and the area-averaged transport coefficient is used in the mass and energy balances. This does not represent the true physics of transport from a fixed particle in a steady unidirectional viscous flow, which is the problem we numerically solved in this work. On the other hand, for a particle in an agitated tank, local variations around the sphere are probably unimportant in the time-averaged result.

Another problem of interest in this study is illustrated by the freezing, or melting, of a spherical ice particle in an aqueous salt solution. Since the solute (salt) is rejected from the ice crystal, the sum of the diffusive and convective fluxes of solute at the particle surface is zero. Thus

$$k(c_s - c_b) - \left(\frac{\rho_s c_s}{\rho_L}\right)\left(\frac{dR}{dt}\right) = 0 \tag{18}$$

and again Equation (15) applies with

$$\alpha = \frac{\rho_s c_s}{\rho_L(c_s - c_b)} \tag{19}$$

There is, however, a difference between this case and those previously discussed. If a dissolution or crystallization process is essentially isothermal and is mass transfer limited, the surface concentration of solute will remain constant. Likewise, if a freezing or melting process involves a pure substance and is heat transfer limited, the surface temperature will remain constant. Therefore, α is constant for such processes, provided that the bulk concentration or temperature is constant; the Nusselt number is then directly proportional to the radial Peclet number, although both will generally vary with time. But when an ice sphere is freezing or melting in a salt solution, the salt concentration at the surface, c_s, will generally vary with time, and α will not be constant. And, of course, the bulk concentration or temperature could be time dependent in any of these processes, depending upon experimental conditions. In the mathematical analysis to follow α will be assumed to be constant. Indeed in transforming Equation (1) to Equation (5) the surface concentration, c_s, and the bulk concentration, c_b, were assumed to be constant. These assumptions may not be met in some experiments, but the results of the analysis are expected to apply, at least approximately, to most situations.

The particle radius divided by its initial value is obtained by integrating the radial Peclet number with respect to dimensionless time, thus

$$\frac{R}{R_i} = \left(1 + \int_o^T N_{PeR}\ dT\right)^{1/2} \tag{20}$$

In solving Equation (5) numerically for spheres of changing radius, Equation (15) was used, with a constant value of α, to relate N_{PeR} to N_{Nu}. Likewise, Equation (20) was used to evaluate changes in R with time. The remaining variable whose time dependence must be established is the flow Peclet number, N_{Pe}. The treatment of this variable is somewhat more arbitrary. It seems experimentally possible to have flow Peclet numbers which vary as a function of time in many ways. For example, one might assume that the particle is exposed to a constant bulk flow velocity and that the Peclet number is therefore

directly proportional to the radius. On the other hand, the particle might be assumed to move at its terminal velocity, and therefore variations in the Peclet number would result from variations in both the velocity and the diameter. This latter assumption seems somewhat more realistic in the description of freely suspended particles, and such a flow Peclet number variation was used to obtain most of the numerical solutions.

The terminal velocity of a sphere is proportional to the diameter raised to the power $(n + 1)/(2 - n)$, where n is the negative slope of the logarithmic curve of drag coefficient versus Reynolds number. Therefore, for a sphere of changing radius which always moves at the free fall terminal velocity corresponding to its instantaneous radius, the bulk flow Peclet number based upon the free fall velocity is given by

$$\frac{N_{Pe}}{(N_{Pe})_i} = \left(\frac{R}{R_i}\right)^{3/2-n} \tag{21}$$

The value of n depends upon the Reynolds number, and thus the solution is dependent upon the Schmidt number as well as the flow Peclet number, since

$$N_{Re} = \frac{N_{Pe}}{N_{Sc}} \tag{22}$$

Numerical solutions were obtained for growing and for shrinking spheres with a Schmidt number of 1,000. Initial values of N_{Pe} and N_{PeR} and the concentration profile were chosen, from which the time-dependent concentration profile and thus the Nusselt number was generated. As the calculation proceeded, N_{PeR} was varied so that it remained in a constant ratio to N_{Nu}, as required by Equation (15). Similarly, R and N_{Pe} were varied as required by Equations (20) and (21). The instantaneous values of N_{Nu}, N_{PeR}, and N_{Pe} which resulted (after the early transient) are plotted in Figures 5 and 6 in normalized coordinates analogous to those of Figures 3 and 4. The normalizing parameter, N_{Nu}^*, is the Nusselt number for $N_{PeR} = 0$, corresponding to steady state transport at the instantaneous value of N_{Pe}. For any numerical calculation, the results traced a path along a 45° line, such as line A-B in Figure 6, as the sphere grew or shrank with a constant ratio of N_{PeR} to N_{Nu}. The cross plots of the results at selected values of N_{Pe}, shown in Figures 5 and 6, were essentially independent of the initial values of N_{Pe}, N_{PeR}, and the initial concentration profile chosen, provided that results of the early part of the transient were discarded. These results are for a specific Schmidt number of 1,000, and they are for the case of no transpiration, which implies that the liquid and solid densities are equal.

An additional numerical solution for a Schmidt number equal to 10 resulted in transport rates which deviated from the solution at the larger Schmidt number by less than 2%. By using a Schmidt number of 1,000, n varied between 0.71 and 1.0, while with the smaller Schmidt number, n ranged between 0.27 and 0.71. Since n must lie between 0 and 1, these results span the range of n values quite well. The insensitivity of the results to this variation in Schmidt number suggests that the results are not greatly dependent upon the manner in which N_{Pe} varies as the sphere shrinks or grows. This was confirmed when a single solution was also obtained for transport from a shrinking sphere exposed to a constant bulk velocity. The solution yielded results which deviated from those in Figure 6 by less than 3%, and therefore the specific nature of the variation of the bulk velocity past the particle apparently has little effect upon the resulting transport.

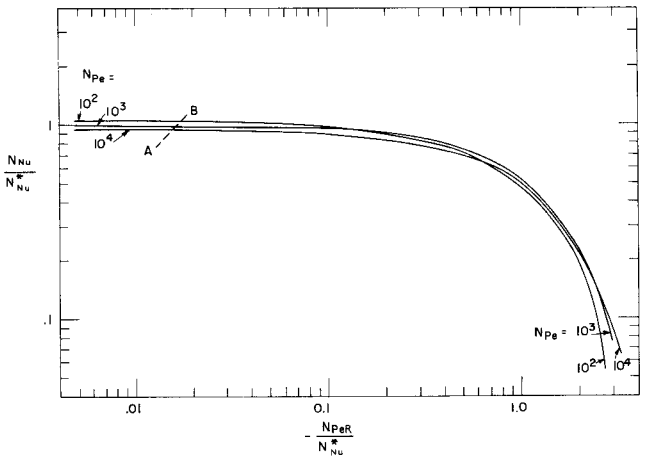

Fig. 6. Transport from a shrinking sphere.

The results in Figures 5 and 6 for growing and shrinking spheres are similar to those in Figures 3 and 4 for transpiring spheres. The effect of N_{Pe} on the normalized presentation of the results is greater in Figures 5 and 6, but at high values of N_{Pe} the sensitivity is not great.

Simultaneous Transpiration and Changing Particle Radius

The shrinking or growing of particles which are not neutrally buoyant results in simultaneous transpiration, and therefore the solution for the combined effects is of interest. Conservation of mass for a melting or dissolution process requires that the transpiring Peclet number be related to the radial Peclet number by

$$N_{PeT} = \left(\frac{\rho_L - \rho_s}{\rho_L}\right) N_{PeR} \tag{23}$$

A single finite-difference solution was obtained in which the radial and transpiring Peclet numbers were both nonzero. Selected results are given in Table 2.

Table 2. Combined Effects of Shrinking and Transpiration

N_{Pe}	N^*_{Nu}	N_{PeR}/N^*_{Nu}	N_{PeT}/N^*_{Nu}	N_{Nu}/N^*_{Nu}
3,000	15.88	—0.795	0.795	0.346
1,000	11.01	—0.803	0.803	0.352

Approximations to these combined transport corrections, N_{Nu}/N_{Nu}^*, can be obtained by assuming that the total correction is the product of the two independent corrections predicted by Figures 4 and 6. When this technique is applied to the two points in Table 2, the results are $N_{Nu}/N_{Nu}^* = 0.58 \times 0.65 = 0.38$ for $N_{Pe} = 3{,}000$, and $N_{Nu}/N_{Nu}^* = 0.60 \times 0.65 = 0.39$ for $N_{Pe} = 1{,}000$. Thus the product of the independent correction factors is seen to be higher than the true correction factor by about 10%.

The results shown in Table 2 were obtained for the radial Peclet number equal to the negative of the transpiring Peclet number, and therefore the solution corresponds to a system in which the solid-liquid density ratio equals two. More important, however, is that by choosing such values, the effects of the transpiration and shrinking are of nearly equal importance, and the error involved in multiplying the two independent correction factors should be a maximum. Therefore, these results suggest that multiplying the independent corrections of Figures 3 or 4 and Figures 5 or 6 will give a reasonably satisfactory approximation to the combined effects of transpiration and a changing particle diameter.

EXPERIMENTAL

Measurements were made of the rate of melting of ice spheres suspended in an agitated tank containing an aqueous sodium chloride solution. A Dewar flask served as the stirred tank. The uniform ice spheres were suddenly introduced into

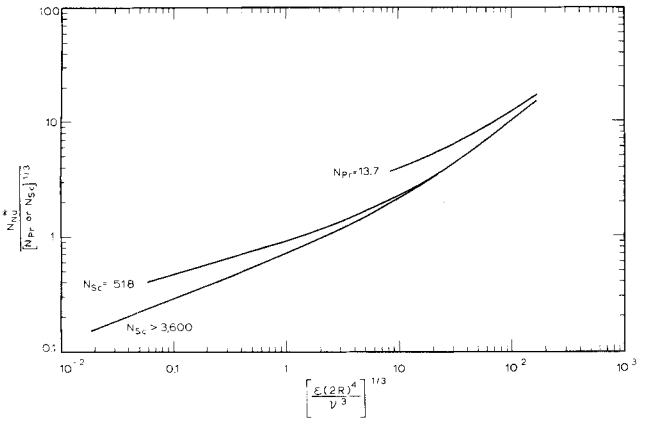

Fig. 7. Correlation of heat and mass transfer coefficients to spherical particles suspended in an agitated liquid, from reference 6.

the agitated, adiabatic tank containing the brine at approximately 0°C. A recording of the transient variation in the bulk brine temperature enabled the calculation of the rate of melting of the ice spheres as a function of their radius as they melted. The apparatus and procedure were identical to those described (*6*) and discussed in greater detail elsewhere (*10*).

When ice spheres are melted in brine, the melting rate is determined both by the heat transfer coefficient and the mass transfer coefficient for salt diffusion. The thermal diffusivity of water is much larger than the mass diffusivity of sodium chloride in water, and therefore the radial and transpiring mass transfer Peclet numbers are much larger than the radial and transpiring heat transfer Peclet numbers. Hence, even though the mass transfer coefficient was reduced substantially by the shrinking of the particle diameter, Figures 3 and 6 predict negligible corrections to the heat transfer coefficient. Consequently, the coefficient of heat transfer from brine to ice spheres was assumed to be that given by the correlation (*6*), reproduced here as Figure 7. The upper curve, for N_{Pr} = 13.7, was obtained by melting ice spheres in pure water (*6*). By using this curve to predict the heat transfer coefficient, the temperature at the particle surface was computed. By assuming that the melting process was heat transfer and salt diffusion-limited, the salt concentration at the particle surface was taken as that in equilibrium with the computed surface temperature. Then the mass transfer coefficient was computed from Equation (18). The computed values of the salt concentration at the particle surface varied with time, but the variation was not great. Therefore α as given by Equation (19) was nearly constant.

RESULTS AND DISCUSSION

Figure 8 shows typical results of the mass-transfer Nusselt number versus particle diameter as the ice spheres melted. The results scatter more than did the heat transfer coefficients which were obtained (*6*) for melting ice spheres in pure water. This is probably due primarily to the loss of precision in the calculation, described above, which is equivalent to subtracting the heat transfer resistance from the total to get the mass transfer resistance. The mass transfer resistance was approximately 50% of the total.

The magnitude of the radial mass transfer Peclet number in these experiments ranged up to 58.7. Since the ice density is 0.906, the transpiring Peclet number is smaller in magnitude, never exceeding 5.5. Both the radial and the transpiring Peclet numbers are negative because the spheres are shrinking and the transpiration velocity is inwardly directed. Therefore, Figures 3 and 6 are the theoretical curves which apply in this case.

Table 3 presents the results of applying the corrections in Figures 3 and 6 to the data in Figure 8. For example, consider the entry for R = 1 mm. (a sphere diameter of 2 mm.). From Figure 7, at the agitation power for the experiment (*6, 10*), the correlation of Reference 6 predicts N_{Nu}^* = 89. The experimental value of N_{PeR} is −42.2, so N_{PeR}/N_{Nu}^* = −0.474. Figure 6 yields a value of N_{Nu}/N_{Nu}^* = 0.64 at N_{PeR}/N_{Nu}^* = −0.474 and N_{Pe} = 2.5 × 10^5. This requires an extrapolation to a bulk flow Peclet number of 2.5 × 10^5. Since, in the turbulent brine in the agitated tank, the bulk flow velocity past the particle was not known, the value N_{Pe} = 2.5 × 10^5 was chosen because at this value, with steady unidirectional flow past a sphere (*10*) at a Reynolds number of approximately 100, N_{Nu}^* = 89 when N_{Sc} = 2,330. The experimental value of N_{PeT} was −4.0, and thus N_{PeT}/N_{Nu}^* = −0.045. The transpiration correction from Figure 3 or Equation (12) is 1.03. Assuming that the independent corrections for shrinking and transpiration may be multiplied, N_{Nu}/N_{Nu}^* = 0.66 according to Figures 3 and 6. Thus the predicted Nusselt number is 0.66 × 89 = 59. The experimental Nusselt number is 59.6, as read from the curve through the data on Figure 8. The agreement between the predicted and experimental Nusselt numbers is quite satisfactory for all entries in Table 3 except the last one, R = 0.4 mm. Even here, where the experimental error is greatest, the deviation is only 21%.

TABLE 3. PREDICTED EFFECT OF SHRINKING AND TRANSPIRATION FOR MELTING OF ICE IN BRINE (N_{Sc} = 2,330)

R (mm.)	N^*_{Nu} (Fig. 7)	N_{PeR} (experimental)	N_{PeT} (experimental)	N_{Nu}/N^*_{Nu} Fig. 6	N_{Nu}/N^*_{Nu} Fig. 3	N_{Nu}/N^*_{Nu} Product of the two	N_{Nu} predicted	N_{Nu} experimental (Fig. 8)
1.2	104	−50.2	−4.7	0.65	1.03	0.67	70	73.4
1.0	89	−42.2	−4.0	0.64	1.03	0.66	59	59.6
0.8	72	−34.2	−3.2	0.64	1.03	0.66	47	46.3
0.6	55	−26.1	−2.5	0.64	1.03	0.66	36	33.7
0.4	39	−21.4	−2.0	0.65	1.03	0.67	26	21.4

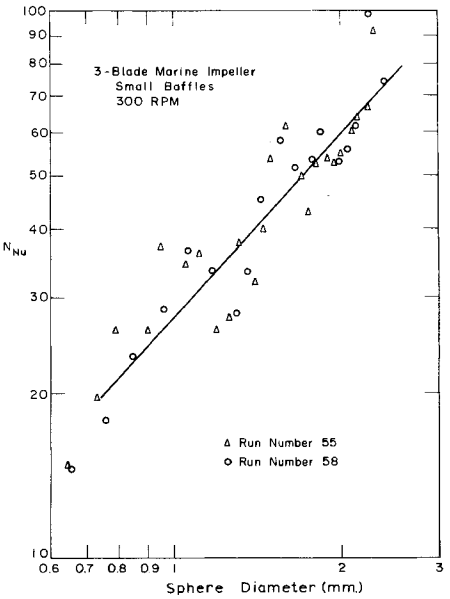

Fig. 8. Mass transfer data (ice-brine).

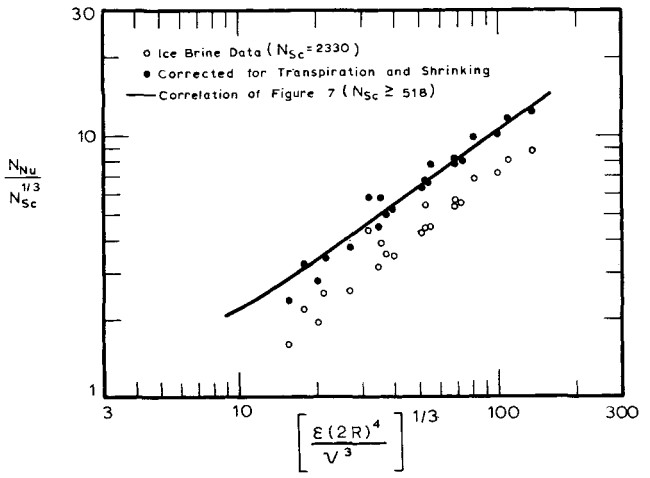

Fig. 9. Ice-brine mass transfer data corrected for transportation and shrinking.

Instead of making the comparison as in Table 3, one could divide the experimental Nusselt number by the correction factor to get $N_{Nu}^* = 59.6/0.66 = 90.3$. This would represent the experimental value corrected for shrinking and transpiration and would be compared with the value of 89 predicted by the general correlation in Figure 7. Figure 9 shows all of the ice-brine mass transfer data corrected in this manner. The curve is that of Figure 7 for $N_{Sc} \geq 518$. The points do not represent actual data points but rather points from smooth curves through the data for different agitation conditions, such as the one shown in Figure 8. The uncorrected points fall below the general correlation, but the corrected points show good agreement with it.

CONCLUSION

Numerical solutions have been obtained for mass or heat transfer to a sphere in a steady laminar flow, with and without transpiration at the sphere surface and a changing diameter of the sphere. Normalized plots of the results are quite insensitive to the bulk flow Peclet number. The results are for steady, unidirectional laminar flow; and the results for a changing particle diameter are restricted to a constant ratio of the Nusselt number to the radial Peclet number. Their applicability to the case of transport to a particle suspended in a turbulent fluid must be assessed by comparison with experiments.

Experimental mass transfer results for ice spheres melting in brine lie below a general correlation (*6, 10*) for transport to spheres in an agitated tank. The theoretical results of this study predict that the shrinking particle diameter and the transpiration should reduce the mass transfer coefficient by a factor of 0.67, in excellent agreement with the experimental results (Figure 9). This agreement suggests that the theoretical curves can be used successfully to predict the effects of transpiration and changing particle diameter for transport to particles suspended in a turbulent fluid.

ACKNOWLEDGMENT

Financial support from the Office of Saline Water, U.S. Department of the Interior, is gratefully acknowledged.

NOTATION

A = inverse dimensionless radial distance, R/r
c = concentration of transferring solute
c_b = concentration of transferring solute in the bulk fluid
c_s = concentration of transferring solute at the particle surface
C_p = specific heat of fluid (liquid)
D = diffusivity (heat or mass)
h = heat transfer coefficient
k_L = local mass transfer coefficient, defined by Equation (7)
k = area-averaged value of k_L
N_{Nu} = Nusselt number, $2Rk/D$ for mass transfer, $2Rh/\rho_L C_p D$ for heat transfer
N_{Nu}^* = Nusselt number at a given bulk flow Peclet number with no transpiration and a constant particle radius
N_{Pe} = bulk flow Peclet number, $2Rv_b/D$
N_{PeR} = radial Peclet number, $(2R/D)(dR/dT)$
N_{PeT} = transpiring Peclet number, $2R(v_r)_s/D$
N_{Re} = $2Rv_b/\nu$
N_{Sc} = Schmidt number, ν/D
R = radius of the sphere
r = radial distance from the center of the sphere
T = dimensionless time, Dt/R_i^2
T_b = temperature of bulk fluid
T_s = temperature at surface of particle
t = time
v_b = bulk velocity of steady unidirectional flow past the sphere
v_r = velocity in the radial direction
v_θ = velocity in the angular direction
X = dimensionless concentration $(c - c_b)/(c_s - c_b)$

Greek Letters

α = N_{Nu}/N_{PeR}, Equation (15)
ϵ = agitation power per unit mass of fluid in agitated tank
θ = angular spherical coordinate
λ = latent heat of fusion
ν = kinematic viscosity of fluid (liquid)
ρ_L = fluid (liquid) density
ρ_s = solid density

Subscripts

i = initial value, at $t = 0$
L = local value at a point on the sphere surface
s = at the particle surface

LITERATURE CITED

1. Acrivos, A., and T. D. Taylor, *Phys. Fluids*, **5**, 387 (1962).
2. Bowman, C. W., D. M. Ward, A. I. Johnson, and O. Trass, *Can. J. Chem. Eng.*, **39**, 9 (1961).
3. Breiman, L., Rpt. No. 2F2, California Inst. Tech., Pasadena, (1952).
4. Brenner, H., *Chem. Eng. Sci.*, **18**, 109 (1963).
5. Brian, P. L. T., *AIChE J.*, **7**, 367 (1961).
6. ———, H. B. Hales, and T. K. Sherwood, "Transport of Heat and Mass Between Liquids and Spherical Particles in an Agitated Tank," *AIChE J.*, to be published.
7. Frank, F. C., *Proc. Roy. Soc. (London) Ser. A*, **201**, 586 (1950).
8. Friedlander, S. K., *AIChE J.* **3**, 43 (1957).
9. *Ibid.*, **7**, 347 (1961).
10. Hales, H. B., Sc.D. thesis Mass. Inst. Tech., Cambridge (1967).
11. Kronig, R., and J. Bruijsten, *Appl. Sci. Research, Sect. A*, **2**, 439 (1951).
12. Levich, V. G., "Physicochemical Hydrodynamics," Prentice-Hall, Englewood Cliffs, N. J. (1962).
13. Mickley, H.S., R. C. Ross, A. L. Squyers, and W. E. Stewart, *Nat. Advisory Comm. Aeron. Tech. Note 3208* (1954).
14. Nielson, A. E., *J. Phys. Chem.*, **65**, 46 (1961).
15. Yuge, T., *Sci. Rept. Res. Inst., Tohoku Univ.*, **6**, 143 (1956).

Manuscript received January 13, 1968; revision received April 3, 1968; paper accepted April 5, 1968.